Computers in Biology and Medicine 108 (2019) 78–84

Contents lists available at ScienceDirect

Computers in Biology and Medicine

journal homepage: www.elsevier.com/locate/compbiomed

Bone and soft tissue changes associated with a removable partial denture. A novel method with a fusion of CBCT and optical 3D images

Marko Kuralt[a,b], Manushaqe Selmani Bukleta[b,c], Milan Kuhar[d,e], Aleš Fidler[f,g,*]

[a] Division of Stomatology, University Medical Centre Ljubljana, Slovenia
[b] Faculty of Medicine, University of Ljubljana, Ljubljana, Slovenia
[c] School of Dentistry, Faculty of Medicine, University of Prishtina, Kosovo
[d] Department of Prosthetic Dentistry, Faculty of Medicine, University of Ljubljana, Slovenia
[e] Department of Prosthodontics, University Medical Centre Ljubljana, Slovenia
[f] Department of Endodontics and Operative Dentistry, Faculty of Medicine, University of Ljubljana, Slovenia
[g] Department of Restorative Dentistry and Endodontics, University Medical Centre Ljubljana, Slovenia

ARTICLE INFO

Keywords:
Cone beam computed tomography
Optical 3D image
Image registration
Image fusion
Removable partial denture
Denture supporting tissue

ABSTRACT

Background: The purpose of this study was to propose a novel method for 3D evaluation of bone and mucosal changes in removable partial denture (RPD) foundation area using a fusion of cone beam computed tomography (CBCT) and optical 3D images.

Method: Two CBCT scans and three impressions, taken at insertion and after ten months of wearing the RPD, were acquired from five patients. 3D models of bone and surface were created from CBCT images and gypsum casts, respectively, spatially aligned and saved in Standard Tessellation Language file format. Visual and numerical analysis of differences between the models allows evaluation of surface, mucosal and bone changes in regions of interest (ROI) defined as narrow ROI (nROI), denture foundation area ROI (dROI) and wide ROI (wROI). Site-specific analysis was performed in mesiodistal and buccolingual direction.

Results: Visual evaluation of 3D color-coded deviation maps showed irregular distribution of bone and surface changes. The differences between mandibles and also between left and right sides were found. Mean volume of bone change in dROI was −135.86 (range = −456.18 to 21.20) mm^3. The average bone change thickness in dROI was −0.26 (range = −0.96 to 0.07) mm. The mean volume changes in nROI were −38.31 (range = −118.26 to 45.87) mm^3, -51.96 (range = −182.54 to 5.6) mm^3 and 13.66 (range = −80.62 to 79.46) mm^3 for surface, bone and mucosa, respectively.

Conclusions: The proposed method facilitates separate visual and numerical evaluation of surface, mucosa and bone changes. It opens possibilities for a better understanding of denture-supporting tissues remodeling, objective evaluation and comparison of different treatment options.

1. Introduction

The resorption of the residual ridge following tooth loss is an irreversible physiological process [1], which can be significantly increased with denture wearing [2]. During wearing a denture, occlusal forces are transferred to denture supporting tissues (DST) [3], consisting of the mucosa, (the submucosa and periosteum), and the underlying bone [4]. The shape and thickness of both soft and mineralized DST form a denture foundation area, a contact area between a denture and mucosal surface [4]. It is a well-known fact that wearing a denture is almost invariably accompanied by undesirable and irreversible morphological changes of DST [4], resulting in poor denture fit with substantial clinical complications [5].

Evaluation of DST morphological changes, associated with wearing a denture, has been studied in the past. The bone changes were evaluated with impressions and casts [6], two-dimensional (2D) radiographic methods including panoramic [7] and cephalometric radiography [8]; and recently with three-dimensional (3D) radiographic methods, using cone beam computed tomography (CBCT) [9–11]. The use of the casts allows evaluation of surface changes only, and consequently, no distinct data for bone and mucosa were available. Radiographic methods are suitable for the evaluation of bone changes only [12]. Use of 2D panoramic and cephalometric radiographic methods was limited by the fact that the 3D structures are shown on the 2D

* Corresponding author. Faculty of Medicine, Department of Endodontics and Operative Dentistry, University of Ljubljana, Vrazov trg 2, 1000, Ljubljana, Slovenia.
E-mail address: ales.fidler@mf.uni-lj.si (A. Fidler).

https://doi.org/10.1016/j.compbiomed.2019.03.024
Received 3 January 2019; Received in revised form 25 March 2019; Accepted 25 March 2019
0010-4825/

image and inherent projection errors [13]. An introduction of 3D imaging techniques overcomes those limitations. A CBCT imaging opens the possibility of 3D evaluation of bone at a much lower radiation dose in contrast to medical CT [14].

In addition to bone changes, denture also can induce mucosal changes – whether decrease (atrophy) or increase (keratinization, hyperplasia) in its thickness [15,16]. In the present literature, there is only one study evaluating the thickness of mandible mucosa in denture foundation area [17] and several studies evaluating the thickness of maxillary mucosa for mucosal graft harvesting purposes [18–21]. Currently, there are no available studies on mucosal changes with time, associated with wearing a denture.

The fusion of computed tomography data and optical 3D images is a new and promising method [22], facilitating 3D evaluation of both hard and soft tissue changes. Recently it has been introduced in maxillofacial - orthognathic surgery and orthodontics [23], implantology [24] and endodontics [25], but not in other areas of dentistry.

The purpose of this study was to propose a novel method for 3D evaluation of bone and mucosal changes in removable partial denture (RPD) foundation area using a fusion of CBCT and optical 3D images.

2. Materials and methods

2.1. Patients selection

This pilot study is a part of a research project and was conducted to validate and improve the methodology of evaluation of prosthodontic treatment with RPD with and without a metal framework on oral health. Ethical approval was obtained from the Ethics Committee of Hospital and University Clinical Service of Kosovo and University Clinical Centre of Kosovo (555/18.05.2017).

The inclusion criteria of patients for the primary study were patients of both genders, aged 45–65 years, Kennedy class I status – a bilateral edentulous area, located posterior to the remaining natural teeth, no previous RPD, prosthodontically unrestored dentition, no caries lesions, and absence of active periodontal disease.

All patients were informed of the protocol of the study, including the two exposures to CBCT and three impressions taken at two time points, and gave their written consent to participate. Image data from first five patients were used to develop a novel method for 3D evaluation of bone and mucosal changes associated with RPD.

2.2. Clinical protocol – 3D data acquisition

All patients eligible for this study had two CBCT scans taken by one experienced radiology technician. The first CBCT scan was taken at insertion of RPD (T1) and the second one after ten months wearing RPD (T2). All CBCT images were taken with the same device (ORTHOPHOS XG 3D; Dentsply Sirona). The exposure parameters were set at 85 kVp, 7 mA for female and 10 mA for male patients, 5 s effective time, 8 × 8 cm field of view and a voxel size of 0,16 mm. The images were acquired and saved in DICOM format for further processing.

Three impressions with irreversible hydrocolloid impression material (XantALGIN Select Fast Set; Heraeus Kulzer GmbH) and perforated stainless steel impression tray (Hi-Tray Metal; Zhermack SpA) were made by one experienced clinician. The impression material was mixed with automatic mixer (Cavex Alginate Mixer II; Cavex Holland BV) using manufacturers recommended mixing ratios between powder and water and using tap water with consistent temperature between 12 and 15-degree Celsius for reproducible consistency and viscosity. Pressure during impression making was controlled in a feedback manner through the clinician sensation. In the cases where the tray was visible or the material thickness was insufficient, the impression was repeated.

The first impression was taken at insertion of RPD (T1) and the second one after ten months wearing RPD (T2). The third impression was taken at T2 together with denture in place to obtain the denture foundation area. Impressions were poured with gypsum immediately after making by a dental technician. Gypsum cast were then digitized with a laboratory scanner (Ceramill Map 400; Amann Girrbach AG) and exported in Standard Tessellation Language (STL) file format.

2.3. Segmentation of 3D bone models from CBCT scans

Segmentation of teeth and bone was performed using implants planning software (RealGUIDE Software version 5.0; 3DIEMME Srl) with “Tooth/Bone Segmentation” software extension. The segmentation procedure is based on graph cuts segmentation technique [26]. It requires selection of the following parameters: bone and background threshold values, bone and background seeds and a smooth factor. The segmentation parameters and minor manual corrections after segmentation were provided by an experienced operator. Both T1 and T2 CBCT images were segmented as described above and stored in STL file format as BONE1 and BONE2, respectively.

2.4. Registration of 3D models

The rigid spatial registration (RealGUIDE Software version 5.0; 3DIEMME Srl) requires manual definition of multiple reference points for initial alignment, which is then automatically refined using best fit matching based on Iterative closest point (ICP) algorithm (Fig. 1) [27].

First BONE1 and BONE2 registration were performed (Fig. 2). As the objects were from different time points, bone structures that were not affected by denture were selected for initial alignment, i.e., left and right mental foramina and mental spine. For refining initial alignment, best fit matching on expanded regions - spheres around initially selected points were used. In the second step, the SURFACE1 and SURFACE2 objects were registered to corresponding bone objects, BONE1 and BONE2, respectively. The structures present in both models were selected for registration between SURFACE and BONE objects from same time, i.e., teeth. Distinct structures like canine cusps and incisal edges were selected for initial alignment. Spheres around those points were then used for refining initial alignment using best fit matching. All four aligned STL objects were exported for further 3D analysis.

2.5. Validation of method reproducibility

The reproducibility of the method may be affected by segmentation of CBCT images and registration process. For the purpose of assessing reproducibility of the method, obtaining 3D bone models, i.e., segmentation of CBCT images, was repeated by the same operater (intra-operater reliability) and by another one (inter-operater reliability). Segmentation of CBCT images was compared with volume-based

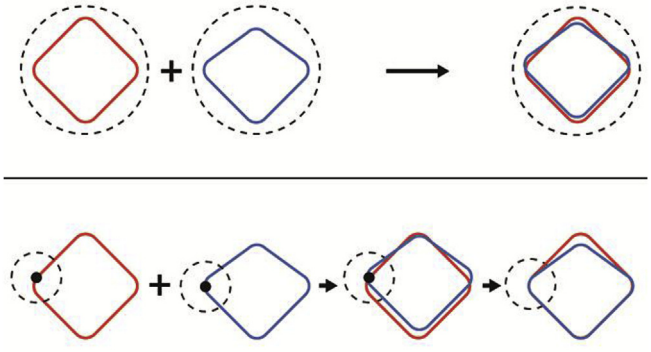

Fig. 1. Comparison of whole object based (upper) and point based (lower) best-fit alignment.

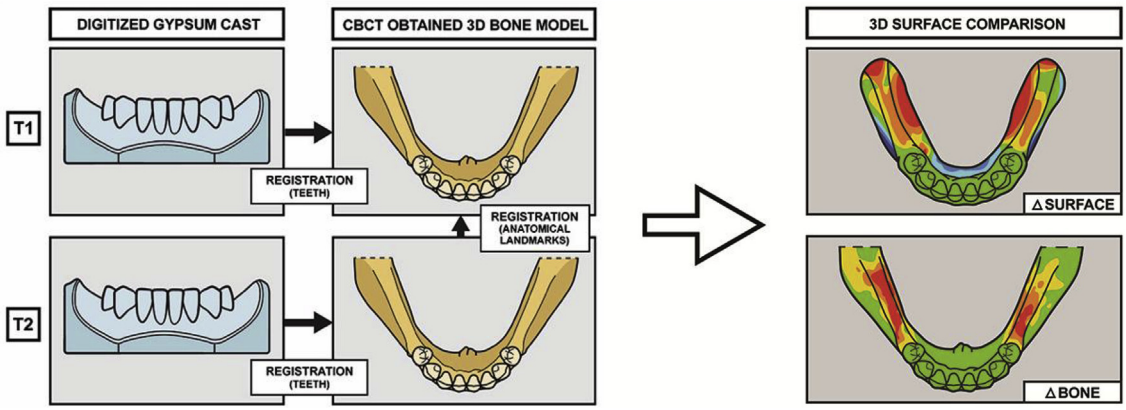

Fig. 2. Surface and bone models registration flowchart. 3D models are obtained with digitizing gypsum casts (surface models) and CBCT segmentation (bone models). Full arrows are showing registration process – SURFACE1 on BONE1 (teeth as registration point) and the same for SURFACE2 on BONE2. So then follows BONE2 on BONE1 registration with already matched corresponding SURFACE models (anatomical landmarks as mental foramina and mental spine as registration point). With aligned 3D models, 3D color-coded deviation maps for surface and bone are created. This enables visual and numerical evaluation of temporal surface and bone changes.

metrics by surface comparison between newly segmented and original 3D models with 3D data measurement analysis software (GOM Inspect 2017; GOM GmbH). Volume values were exported into a statistical software program (IBM SPSS Statistics version 25; IBM Corp) where intra- and inter-operater reliability were assessed by the intra-class correlation coefficient (ICC).

BONE1 to BONE2 registration and SURFACE to BONE registration was repeated by the same operater (intra-operater reliability) and by another one (inter-operater reliability) as well. In BONE1 to BONE2 registrations, mean absolute deviations between the two 3D objects were calculated in 4 regions on stable areas where no change was expected and in 4 regions where change was expected, i.e., alveolar ridge, 8 regions total. In SURFACE to BONE registration, mean absolute deviations between the two 3D objects were calculated in 4 regions on alveolar ridge. Deviation values between compared models were exported into a statistical software program (IBM SPSS Statistics version 25; IBM Corp). Intra- and inter-operater reliability for the measurements - mean absolute deviations were assessed by the ICC.

2.6. Analysis of aligned 3D models

The DST changes were quantified with 3D data measurement analysis software (GOM Inspect 2017; GOM GmbH). Visual evaluation was facilitated by the design of 3D color-coded deviations maps obtained by calculating the Euclidean distances between previously aligned 3D STL models, obtained with the same modality. The areas with changes within the arbitrary set threshold limit of ± 0.5 mm were displayed in green, areas with loss were presented with increasingly saturated red and areas with gain were presented by increasingly saturated blue. Additionally, a denture foundation area, obtained from impression with a denture, was marked in 3D images with a line. Two 3D color-coded deviation maps, one for surface (SURFACE) and one for bone changes (BONE) were created (Fig. 3). Such images enable visualization and descriptive analysis of temporal differences between the two 3D models.

Three regions of interest (ROI) were defined for numerical evaluation. Beside denture foundation area ROI (dROI), defined with denture borders, wide (wROI) and narrow (nROI) ROI were selected (Fig. 4).

The numerical evaluation was performed for the left and right side separately. The area of surface dROI was measured and expressed in mm^2. Bone volume changes were measured in wROI and dROI and expressed in mm^3. A volume to surface ratio was calculated, reporting the average bone change thickness in dROI. Percentage of bone changes within dROI was calculated as well. Bone and soft tissue volume

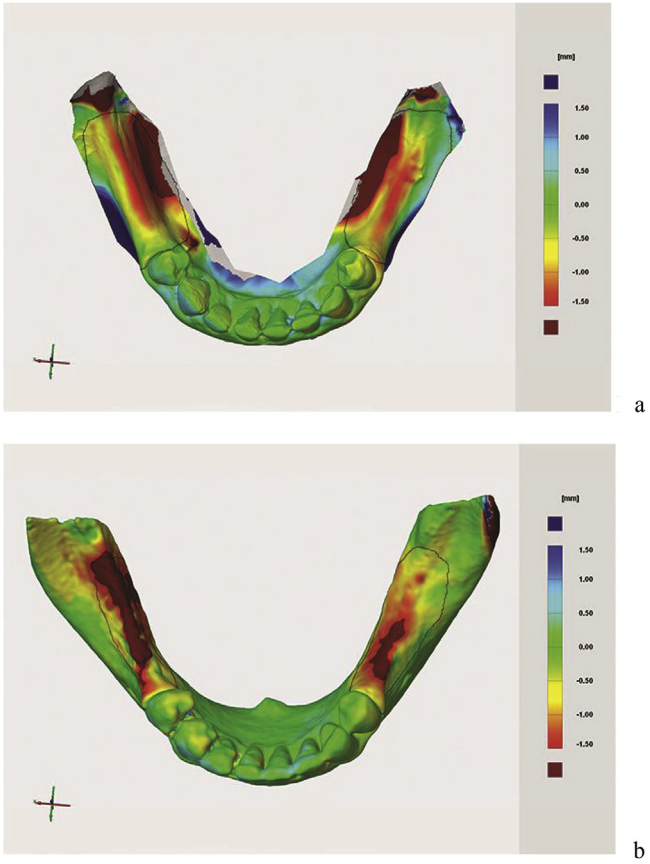

Fig. 3. 3D color-coded deviation maps for surface (a) and bone changes (b).

changes were measured and performed at nROI. Positive values represent gain while negative values represent a loss of tissue. For the nROI we assume that the surface changes are a sum of bone changes and mucosal changes, $dV_{surface} = dV_{mucosa} + dV_{bone}$; therefore, the mucosa volume changes were calculated as $dV_{mucosa} = dV_{surface} - dV_{bone}$. All data was saved to a statistical software program (IBM SPSS Statistics version 25; IBM Corp).

Visual evaluation of 3D color-coded deviation maps revealed site-specific changes. Evaluation of changes in mesiodistal direction was calculated in cross-sections, with a distance of 0.5 mm. Values of changes from nROI were exported into spreadsheet software (Microsoft

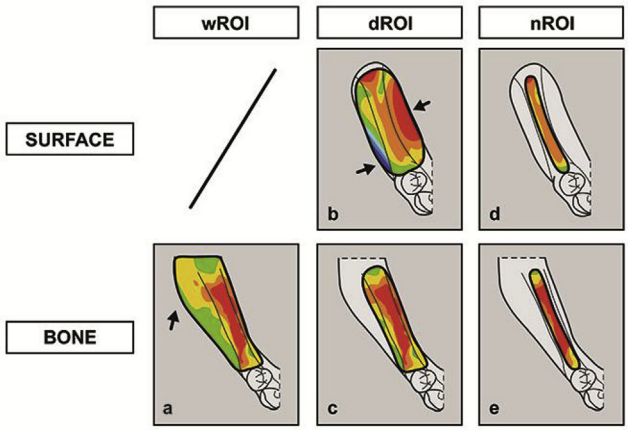

Fig. 4. Regions of interest (ROI) for numerical analysis. First, denture foundation area ROI (dROI) was defined with denture borders on the surface 3D color-coded deviation map (b). dROI on bone 3D color-coded deviation map (c) was defined with the 3D data analysis software-based projection of the denture borders perpendicular to bone surface. Extreme changes due to the mobility of loosely attached alveolar lining mucosa (arrows on b) in denture foundation area were the reason that narrow region (nROI) on central residual ridge area, limited to a firmly attached masticatory mucosa in width of 4 mm was defined, on both surface (d) and bone (e) 3D color-coded deviation maps to avoid misleading data. Bone changes were also present out of the denture foundation area on the bone 3D color-coded deviation map (arrow on a). Therefore, a wider ROI, including all bone changes was defined and referred to as wROI. wROI is defined with last remaining tooth mesially, mylohyoid line medially, laterally oblique line of the mandible and mental foramen laterally, and the transition to ramus distally. Due to the extreme changes caused by the mobility of loosely attached alveolar lining mucosa already in dROI, wROI was not selected on surface model to avoid misleading data.

Excel for Mac version 16; Microsoft). For each cross-section mean change was calculated and exported to a statistical software program. Plots with showing change of surface, mucosa, and bone were created and aligned with color-coded 3D deviation maps (Fig. 5). The positive values represent gain in mucosa thickness, the negative values represent loss in mucosa thickness, while 0 indicates that there was no change in mucosa thickness.

For a further understanding of the site-specific relationship between surface, mucosa and bone changes, buccolingual cross-sections were designed at several specific sites. Such cross-sections facilitate measurement of surface, mucosa and bone changes at each point. (Fig. 5).

3. Results

Visual evaluation of 3D color-coded deviation maps of surface and bone models revealed a high diversity of surface and bone changes. Bone models revealed differences between mandibles and also between left and right residual ridge within each mandible. Bone models mostly exhibited no change or small bone loss in restricted parts of the residual ridges, except for mandible 1 and 4, in which extensive bone loss was found. Surface models show even more diversity. Areas exhibiting loss, no change and gain were found in surface models. The biggest changes, both gain and loss were found at the borders of all surface models.

The surface area of denture foundation area of surface models and volumetric changes of bone models in dROI and wROIs are shown in Table 1. Mean surface area of denture foundation area was 499.69 (range = 317.47 to 719.50) mm^2. Mean bone volume change in dROI was −135.86 (range = −456.18 to 21.20) mm^3. Mean bone volume change in wROI was −183.10 (range = −713.38 to 78.28) mm^3. Comparison between bone changes in dROI and wROI revealed that on average 59.60% (range = −12%–113%) of all bone changes occurred inside dROI.

Volumetric changes in nROI for right and left side are shown in Table 2. Mean changes were −38.31 (range = −118.26 to 45.87) mm^3, -51.96 (range = −182.54 to 5.6) mm^3 and 13.66 (range = −80.62 to 79.46) mm^3 for surface, bone and mucosa, respectively.

Average bone change thickness in dROI and nROI are shown in Table 3. Average bone change thickness was −0.26 (range = −0.96 to 0.07) mm in dROI and −0.42 (range = −1.73 to 0.06) in nROI.

Evaluation of changes in mesiodistal direction and on buccolingual cross-sections show site-specific changes (Fig. 5). Mucosa thickness exhibited loss as well as gain, depending on site.

Results of method validation shows excellent intra- and inter-operater reliability for segmentation and registration and are shown in Table 4.

4. Discussion

The proposed method, using a fusion of CBCT and optical 3D images, offers a 3D evaluation of distinct bone and mucosal changes in denture foundation area. Evaluation of those changes can be visual, based on 3D color-coded deviation maps, and numerical, facilitating measurement of thickness, area, and volume.

The originality of the present method is the fusion of 3D image data acquired with two different modalities that were acquired at two time points. Such fusion requires precise spatial registration of four objects in STL file format. The adequately selected sequence of registration together with a selection of representative reference points is crucial for alignment of 3D models. Stable anatomical landmarks outside the denture foundation area were selected for the registration of bone objects (BONE1 to BONE2), because of their resistance to temporal changes. For registration of surface models to previously registered corresponding bone models (SURFACE1 to BONE1 and SURFACE2 to BONE2), teeth are the only possible structures for registration, as they are represented in both 3D objects, limiting the method to partially edentulous patients only. In order to achieve optimal registration, the reference points should be as distant as possible. Automated best fit registration based on ICP algorithm was used in this study, requiring an operator selected reference point and sphere size selection. The method is based on the principle that human is better at coarse alignment, while the computer is better at fine alignment within the sphere. Instead of best fit alignment on the whole surface of 3D models, aiming to minimize the difference between the two 3D models, the limited regions, representing the stable area, were selected (Fig. 1). Furthermore, using the best fit registration based on ICP algorithm minimizes intra- and inter-operater variability due to insensitivity to small variations in reference point positioning [27,28]. This is achieved as long as corresponding reference points are positioned within the user-defined sphere, in other words, the inter- and intra-operater variability should be within sphere limits. In our study, the sphere diameter was set to 1 cm, which is well above inter- and intra-operater variability, proved with excellent ICC values.

The numerical evaluation was performed in three different ROI (Fig. 4). The dROI was an obvious decision because we aimed to quantify changes under the denture. A visual evaluation revealed two phenomena. Firstly, extensive bone changes were observed at and even outside the denture foundation area border of bone model. Therefore, a wROI was selected for bone volume changes evaluation. Secondly, extensive surface changes were observed at the lingual and buccal borders of the 3D surface model. They resulted from high mobility of loosely attached alveolar lining mucosa in these areas. The loosely attached alveolar lining mucosa was also found at the denture foundation area borders, progressively transforming into a firmly attached masticatory mucosa at the central part of the narrow region of the central ridge. Therefore, a nROI, limited to a firmly attached masticatory mucosa in width of 4 mm in a central ridge area, was necessary.

Beside of one-dimensionally measurements limited to arbitrarily

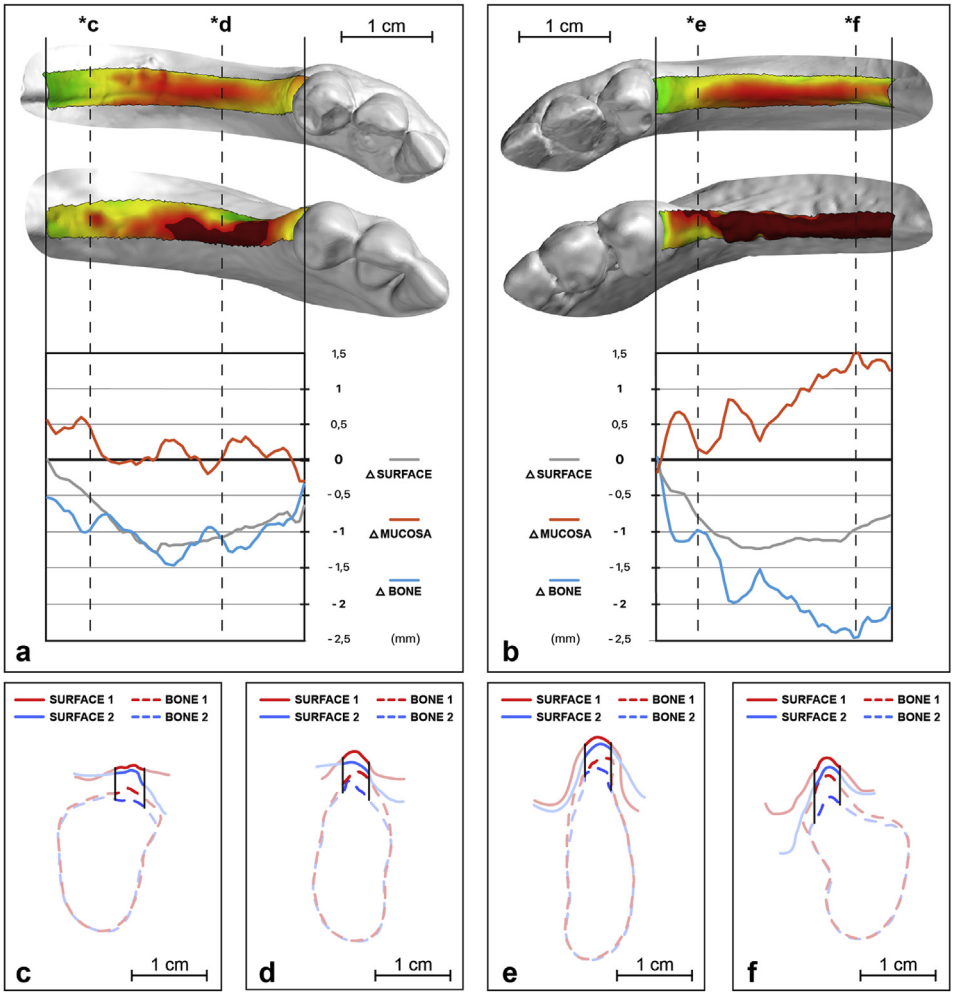

Fig. 5. Evaluation of changes in mesiodistal direction and on buccolingual cross-sections for mandible No. 1. Changes in mesiodistal direction for left (a) and right (b) residual ridges are displayed with, 3D color-coded deviation map of the surface (top image) and bone (middle image), and with a plot with average changes of thickness for surface, mucosa and bone (bottom image) along the left and right alveolar ridge. It should be noted that the positive values represent gain in mucosa thickness, the negative values represent loss in mucosa thickness, while 0 indicates that there was no change in mucosa thickness. Vertical lines, marked with (*c, *d, *e, and *f) are indicating positions of corresponding buccolingual cross-section images (c, d, e, and f). Black vertical lines in cross-section images indicate narrow ROI (nROI) borders.

Table 1
Results of bone changes in five mandibles, separate for left and right side.

No.	side	Denture foundation area (mm^2)	ΔVolume in dROI (mm^3)	ΔVolume in wROI (mm^3)	ΔVolume within dROI (%)
1	right	473.06	−456.18	−713.38	64
	left	424.83	−317.08	−405.36	78
2	right	479.97	20.07	25.78	78
	left	348.88	−59.78	−147.45	41
3	right	481.96	−72.48	−90.81	80
	left	692.34	−9.29	78.28	−12 *
4	right	694.80	−109.59	−96.75	113 **
	left	719.50	−370.20	−527.08	70
5	right	317.47	21.20	56.98	37
	left	364.07	−5.30	−11.20	47

ΔVolume within dROI was calculated as ΔVolume in dROI/ΔVolume in wROI and represents percentage of bone change occurred within dROI.
* ΔVolume in dROI was negative value, while ΔV in wROI was positive value, resulting in negative percentage value.
** ΔV in dROI was bigger than ΔV in wROI, due to bone gain outside dROI, resulting in percentage, higher than 100%.

Table 2
Volumetric changes in nROI at right and left residual ridge for surface, bone, and mucosa.

	side	ΔVolume surface (mm^3)	ΔVolume bone (mm^3)	ΔVolume mucosa (mm^3)
1	right	−103.08	−182.54	79.46
	left	−108.29	−138.12	29.83
2	right	−33.34	0.27	−33.61
	left	−118.26	−37.64	−80.62
3	right	11.83	−24.68	36.51
	left	45.87	−15.47	61.34
4	right	−49.00	−40.87	−8.13
	left	−49.09	−86.99	37.90
5	right	−18.89	0.84	−19.73
	left	39.20	5.60	33.60

defined sites only [10], this method enables advanced numerical evaluation of surface and volume. Volume was rarely used as a parameter in describing the dynamics of DST in previous studies. The bone change was presented as a percentage of total mandible volume [11]. Such parameter depends not only on bone volume change itself but also on whole mandible volume, rendering between subject comparison difficult. Besides reporting the absolute volumes, for left and right side, a volume to surface ratio was calculated, reporting the average thickness of bone loss in denture foundation area. This parameter allows comparison between denture foundation areas of different sizes.

Results of changes after ten months show variability between the subjects, between left and right sides and most importantly high within ROI variability. We found that predominantly bone loss or no change were present. Interestingly, some bone gain was also found in small areas, confirming the result of the previous study, where bone changes, including bone gain, were described and explained as remodeling phenomenon, i.e., resorption and deposition of bone tissues [11]. Interestingly, bone loss was not limited only to the denture foundation area (dROI). Areas of considerable bone loss were in some cases

Table 3
Average bone change thickness at dROI and nROI.

	side	dROI (mm)	nROI (mm)
1	right	−0.96	−1.73
	left	−0.75	−0.97
2	right	0.04	0.01
	left	−0.17	−0.20
3	right	−0.15	−0.21
	left	−0.01	−0.11
4	right	−0.16	−0.32
	left	−0.51	−0.72
5	right	0.07	0.01
	left	−0.01	0.06

Table 4
Intra-class correlation coefficients (ICC) to test the repeatabilty of the presented method within operater (intra) and between operaters (inter).

Operater relation	Segmentation	Registration (BONE1 – BONE 2)	Registration (SURFACE - BONE)
Intra	0.997	0.923	0.933
Inter	0.995	0.895	0.915

extending outside of denture foundation area as seen on Fig. 3b. This might be explained by a pressure related bone resorption, caused by denture margins. Obviously, the process is gradually diminishing instead of being sharply limited. As direct comparison of bone volume changes at dROI and nROI is not relevant due to the differences of surface areas of dROI and nROI. the average bone change thickness was introduced for comparison. It shows that either more bone remodeling occurred on the top of the residual ridge compared to its sides or that the bone remodeling was similar under whole denture foundation area. The high site variability suggests that bone remodeling is a site-specific process, unequally affecting the bone surface.

Changes in mucosa thickness couldn't be visualized like surface and bone changes with 3D color-coded deviation maps. For qualitative evaluation a simultaneous comparison of surface and bone changes models could be used as in Fig. 5a. For quantitative evaluation we proposed to solve this with simple equation "$dV_{mucosa} = dV_{surface} - dV_{bone}$" or with using cross-section analysis. With this in mind, nROI located on firmly attached masticatory mucosa was selected. Evaluation of nROI revealed that bone changes are well compensated by either decrease or increase in mucosa thickness, resulting in a reduction of surface morphology change. Again, this observation shows site-specific variability.

In the present study, image data were acquired by two methods – digitizing gypsum casts and CBCT imaging. Digitizing gypsum casts with the laboratory scanner is a validated method, producing accurate 3D surface models [29,30]. The accuracy of a gypsum cast is influenced by impression taking, i.e., selection of impression material, tray and impression technique, compression of mucosa, and gypsum cast pouring [31]. For obtaining accurate surface information the viscoelastic rheological properties of impression material are very important [32]. In our method, irreversible hydrocolloid impression material was used, which requires significant pressure to record the alveolar ridge. However, being hydrophilic in nature, it provides good contact with wet surface of oral mucosa. To achieve intimate contact between impression and oral mucosa at smallest possible loading, viscosity was reduced with automatic mixing [33]. Oral mucosa is highly deformable under compression. Compression might lead to inaccuracy of measurements in mucosa thickness and surface changes. However, this deformation is highly site specific [17], which is very clearly seen in 3D color-coded deviation maps for surface changes in Fig. 4 in areas with loosely attached alveolar lining mucosa, i.e., the borders of the surface comparison models. Regions with firmly attached masticatory mucosa are more resistant under compression and this is also why a region limited to a firmly attached masticatory mucosa (nROI), was selected for analysis, which proved to be accurate enough with irreversible hydrocolloid impression material [34]. Intraoral scanning would omit these factors and seems a superior technique. Unfortunately, edentulous areas are lacking anatomic mucosal landmarks [35] and factors like lack of space, patient movement, saliva flow and humidity [36], rendering intraoral scanning less reliable and suitable for this task.

3D bone models were obtained by automated segmentation of CBCT images. The most often used CT image segmentation method in medicine is thresholding, which often requires extensive manual post-processing [37]. In our study a graph cuts segmentation technique was used, requiring an operator selected threshold values and seed points. Although the CBCT is inferior compared to medical CT regarding the stability and reliability of voxel values, due to errors of reconstruction algorithm and artifacts [38], the benefits of CBCT, such as small voxel size, isotropic voxel, and lower dose [39], warrant its use in such studies. With additional seed points selection beside threshold setting, graph cuts segmentation is advanced thresholding approach, which reduces manual post-processing and increases accuracy [26].

Visual representation of comparisons between surface and bone models enables a thorough analysis of the dynamics in DST. 3D color-coded deviation maps show the areas, exhibiting changes as well as the magnitude of changes, represented by hue.

5. Conclusion

Wearing dentures is accompanied by undesirable and irreversible morphological changes of DST [4]. The proposed method facilitates separate evaluation of surface, mucosa and bone changes with a fusion of computed tomography data and optical 3D images. Visual and numerical evaluation of DST opens possibilities for a better understanding of DST remodeling, objective evaluation, and comparison of different treatment options.

Declarations of interest

None.

Acknowledgements

The work was supported by the Ministry of Higher Education, Science and Technology of the Republic of Slovenia, under grant number P3-0293.

The authors thank 3DIEMME Srl., for providing the RealGUIDE Software version 5.0.

References

[1] S. Hansson, A. Halldin, Alveolar ridge resorption after tooth extraction: a consequence of a fundamental principle of bone physiology, J. Dent. Biomech. 3 (2012) 1758736012456543 https://doi.org/10.1177/1758736012456543.
[2] A. Tallgren, The continuing reduction of the residual alveolar ridges in complete denture wearers: a mixed-longitudinal study covering 25 years, J. Prosthet. Dent 89 (1972) 427–435 https://doi.org/10.1016/S0022391303001586.
[3] J. Zmudzki, G. Chladek, J. Kasperski, Biomechanical factors related to occlusal load transfer in removable complete dentures, Biomechanics Model. Mechanobiol. 14 (2015) 679–691 https://doi.org/10.1007/s10237-014-0642-0.
[4] L. Kumar, Biomechanics and clinical implications of complete edentulous state, J. Clin. Gerontol. Geriatr. 5 (2014) 101–104 https://doi.org/10.1016/j.jcgg.2014.03.001.
[5] M. Saito, K. Notani, Y. Miura, T. Kawasaki, Complications and failures in removable partial dentures: a clinical evaluation, J. Oral Rehabil. 29 (2002) 627–633 https://doi.org/10.1046/j.1365-2842.2002.00898.x.
[6] I.R. Blum, J.F. McCord, A clinical investigation of the morphological changes in the posterior mandible when implant-retained overdentures are used, Clin. Oral Implant. Res. 15 (2004) 700–708 https://doi.org/10.1111/j.1600-0501.2004.01057.x.
[7] M.A. Elsyad, S.S. Mohamed, A.F. Shawky, Posterior mandibular ridge resorption associated with different retentive systems for overdentures: a 7-year retrospective preliminary study, Int. J. Prosthodont. (IJP) 30 (2017) 260–265 https://doi.org/10.

11607/ijp.5114.
[8] J.W. Unger, C.W. Ellinger, J.C. Gunsolley, An analysis of the effect of mandibular length on residual ridge loss in the edentulous patient, J. Prosthet. Dent 67 (1992) 827–830.
[9] C.R. Moreira, M.A. Sales, P.M. Lopes, M.G. Cavalcanti, Assessment of linear and angular measurements on three-dimensional cone-beam computed tomographic images, Oral Surg. Oral Med. Oral Pathol. Oral Radiol. Endod. 108 (2009) 430–436 https://doi.org/10.1016/j.tripleo.2009.01.032.
[10] O. Ozan, K. Orhan, S. Aksoy, M. Icen, B. Bilecenoglu, B.U. Sakul, The effect of removable partial dentures on alveolar bone resorption: a retrospective study with cone-beam computed tomography, J. Prosthodont. 22 (2013) 42–48 https://doi.org/10.1111/j.1532-849X.2012.00877.x.
[11] R. Ahmad, M.I. Abu-Hassan, Q. Li, M.V. Swain, Three dimensional quantification of mandibular bone remodeling using standard tessellation language registration based superimposition, Clin. Oral Implant. Res. 24 (2013) 1273–1279 https://doi.org/10.1111/j.1600-0501.2012.02566.x.
[12] A.M. Timock, V. Cook, T. McDonald, M.C. Leo, J. Crowe, B.L. Benninger, et al., Accuracy and reliability of buccal bone height and thickness measurements from cone-beam computed tomography imaging, Am. J. Orthod. Dentofacial Orthop. 140 (2011) 734–744 https://doi.org/10.1016/j.ajodo.2011.06.021.
[13] A. Suomalainen, E. Pakbaznejad Esmaeili, S. Robinson, Dentomaxillofacial imaging with panoramic views and cone beam CT, Insights Imaging 6 (2015) 1–16 https://doi.org/10.1007/s13244-014-0379-4.
[14] J.A. Roberts, N.A. Drage, J. Davies, D.W. Thomas, Effective dose from cone beam CT examinations in dentistry, Br. J. Radiol. 82 (2009) 35–40 https://doi.org/10.1259/bjr/31419627.
[15] M.K. Razek, N.A. Shaaban, Histochemical and histopathologic studies of alveolar mucosa under complete dentures, J. Prosthet. Dent 39 (1978) 29–36 https://doi.org/10.1016/S0022-3913(78)80042-0.
[16] R.J. Cook, Response of the oral mucosa to denture wearing, J. Dent. 19 (1991) 135–147 https://doi.org/10.1016/0300-5712(91)90001-F.
[17] J. Dong, F.Y. Zhang, G.H. Wu, W. Zhang, J. Yin, Measurement of mucosal thickness in denture-bearing area of edentulous mandible, Chin. Med. J. (Engl). 128 (2015) 342–347 https://doi.org/10.4103/0366-6999.150100.
[18] A. Heil, F.S. Schwindling, C. Jelinek, M. Fischer, M. Prager, E. Lazo Gonzalez, et al., Determination of the palatal masticatory mucosa thickness by dental MRI: a prospective study analysing age and gender effects, Dentomaxillofacial Radiol. 47 (2018) 20170282 https://doi.org/10.1259/dmfr.20170282.
[19] H.P. Muller, N. Schaller, T. Eger, Ultrasonic determination of thickness of masticatory mucosa: a methodologic study, Oral Surg. Oral Med. Oral Pathol. Oral Radiol. Endod. 88 (1999) 248–253 https://doi.org/10.1016/S1079-2104(99)70123-X.
[20] J.E. Song, Y.J. Um, C.S. Kim, S.H. Choi, K.S. Cho, C.K. Kim, et al., Thickness of posterior palatal masticatory mucosa: the use of computerized tomography, J. Periodontol. 79 (2008) 406–412 https://doi.org/10.1902/jop.2008.070302.
[21] N. Wara-aswapati, W. Pitiphat, N. Chandrapho, C. Rattanayatikul, N. Karimbux, Thickness of palatal masticatory mucosa associated with age, J. Periodontol. 72 (2001) 1407–1412 https://doi.org/10.1902/jop.2001.72.10.1407.
[22] E. Nkenke, E. Vairaktaris, F.W. Neukam, A. Schlegel, M. Stamminger, State of the art of fusion of computed tomography data and optical 3D images, Int. J. Comput. Dent. 10 (2007) 11–24.
[23] J.M. Plooij, T.J. Maal, P. Haers, W.A. Borstlap, A.M. Kuijpers-Jagtman, S.J. Berge, Digital three-dimensional image fusion processes for planning and evaluating orthodontics and orthognathic surgery. A systematic review, Int. J. Oral Maxillofac. Surg. 40 (2011) 341–352 https://doi.org/10.1016/j.ijom.2010.10.013.
[24] B. Yilmaz, Incorporating digital scans of diagnostic casts into computed tomography for virtual implant treatment planning, J. Prosthet. Dent 114 (2015) 178–181 https://doi.org/10.1016/j.prosdent.2015.03.009.
[25] W.J. van der Meer, A. Vissink, Y.L. Ng, K. Gulabivala, 3D Computer aided treatment planning in endodontics, J. Dent. 45 (2016) 67–72 https://doi.org/10.1016/j.jdent.2015.11.007.
[26] Y. Boykov, G. Funka-Lea, Graph cuts and efficient N-D image segmentation, Int. J. Comput. Vis. 70 (2006) 109–131 https://doi.org/10.1007/s11263-006-7934-5.
[27] P.J. Besl, N.D. McKay, A method for registration of 3-D shapes, IEEE Trans. Pattern Anal. Mach. Intell. 14 (1992) 239–256 https://doi.org/10.1109/34.121791.
[28] S. Rusinkiewicz, M. Levoy, Efficient variants of the ICP algorithm, Proc 3rd Int Conf 3-D Digital Imaging Modeling (2001) 145–152 https://doi.org/10.1109/IM.2001.924423.
[29] A. Ender, T. Attin, A. Mehl, In vivo precision of conventional and digital methods of obtaining complete-arch dental impressions, J. Prosthet. Dent 115 (2016) 313–320 https://doi.org/10.1016/j.prosdent.2015.09.011.
[30] C. Kirschnecka, B. Kamufb, C. Putschb, S. Chhatwanib, M. Bizhangc, G. Daneshb, Conformity, reliability and validity of digital dental models created by clinical intraoral scanning and extraoral plaster model digitization workflows, Comput. Biol. Med. 100 (2018) 114–122 https://doi.org/10.1016/j.compbiomed.2018.06.035.
[31] S. Thongthammachat, B.K. Moore, M.T. Barco 2nd, S. Hovijitra, D.T. Brown, C.J. Andres, Dimensional accuracy of dental casts: influence of tray material, impression material, and time, J. Prosthodont. 11 (2002) 98–108 https://doi.org/10.1053/jopr.2002.125192.
[32] M. Kawara, M. Iwasaki, Y. Iwata, Y. Komoda, S. Inoue, O. Komiyama, et al., Rheological properties of elastomeric impression materials for selective pressure impression technique, J. Prosthodont. Res. 59 (2015) 254–261 https://doi.org/10.1016/j.jpor.2015.07.002.
[33] K. Inoue, Y.X. Song, O. Kamiunten, J. Oku, T. Terao, K. Fujii, Effect of mixing method on rheological properties of alginate impression materials, J. Oral Rehabil. 29 (2002) 615–619 https://doi.org/10.1046/j.1365-2842.2002.00726.x_C.
[34] T. Matsuda, T. Goto, K. Kurahashi, T. Kashiwabara, M. Watanabe, Y. Tomotake, et al., Digital assessment of preliminary impression accuracy for edentulous jaws: comparisons of 3-dimensional surfaces between study and working casts, J. Prosthodont. Res. 60 (2016) 206–212 https://doi.org/10.1016/j.jpor.2015.12.007.
[35] F.S. Andriessen, D.R. Rijkens, W.J. van der Meer, D.W. Wismeijer, Applicability and accuracy of an intraoral scanner for scanning multiple implants in edentulous mandibles: a pilot study, J. Prosthet. Dent 111 (2014) 186–194 https://doi.org/10.1016/j.prosdent.2013.07.010.
[36] F. Kuhr, A. Schmidt, P. Rehmann, B. Wostmann, A new method for assessing the accuracy of full arch impressions in patients, J. Dent. 55 (2016) 68–74 https://doi.org/10.1016/j.jdent.2016.10.002.
[37] M. van Eijnatten, R. van Dijk, J. Dobbe, G. Streekstra, J. Koivisto, J. Wolff, CT image segmentation methods for bone used in medical additive manufacturing, Med. Eng. Phys. 51 (2018) 6–16 https://doi.org/10.1016/j.medengphy.2017.10.008.
[38] R. Schulze, U. Heil, D. Gross, D.D. Bruellmann, E. Dranischnikow, U. Schwanecke, et al., Artefacts in CBCT: a review, Dentomaxillofacial Radiol. 40 (2011) 265–273 https://doi.org/10.1259/dmfr/30642039.
[39] T. Kiljunen, T. Kaasalainen, A. Suomalainen, M. Kortesniemi, Dental cone beam CT: a review, Phys. Med. 31 (2015) 844–860 https://doi.org/10.1016/j.ejmp.2015.09.004.